Electronic Supplementary Material (ESI) for Journal of Materials Chemistry C

Supporting information

A simple carbazole-N-benzimidazole bipolar host material for highly efficient blue and single layer white phosphorescent organic light-emitting diodes

Biao Pan,[a] Bo Wang,[a] Yixing Wang,[a] Peng Xu,[a] Lei Wang,*[a] Jiangshan Chen*[b], Dongge Ma[b]

[a]Wuhan National Laboratory for Optoelectronics, School of Optical and Electronic Information Huazhong University of Science and Technology,Wuhan, 430074, P. R. China
E-mail: wanglei@mail.hust.edu.cn
[b]State Key Laboratory of Polymer Physics and Chemistry, Changchun Institute of Applied Chemistry, Chinese Academy of Sciences, Changchun, 130022, P. R. China
E-mail: jschen@ciac.ac.cn

Experimental Section

General information

All solvents and materials were used as received from commercial suppliers without further purification. Synthetic routes of the benzimidazole derivatives are outlined in Scheme S1. ^{1}H NMR and ^{13}C NMR spectra were measured on a Bruker-AF301 AT 400MHz spectrometer. Elemental analyses of carbon, hydrogen, and nitrogen were performed on an Elementar (Vario Micro cube) analyzer. Mass spectra were carried out on an Agilent (1100 LC/MSD Trap) using ACPI ionization. UV-Vis absorption spectra were recorded on a Shimadzu UV-VIS-NIR Spectrophotometer (UV-3600). PL spectra were recorded on Edinburgh instruments (FLSP920 spectrometers). Differential scanning calorimetry (DSC) was performed on a PE Instruments DSC 2920 unit at a heating rate of 10 ℃/min from 30 to 250 ℃ under nitrogen. The glass transition temperature (T_g) was determined from the second heating scan. Thermogravimetric analysis (TGA) was undertaken with a PerkinElmer Instruments (Pyris1 TGA). The thermal stability of the samples under a nitrogen atmosphere was determined by measuring their weight loss while heating at a rate of 10 ℃/min from 30 to 700 ℃. Cyclic voltammetry measurements were carried out in a conventional three electrode cell using a Pt button working electrode of 2 mm in diameter,

a platinum wire counter electrode, and a $Ag/AgNO_3$ (0.1 M) reference electrode on a computer-controlled EG&G Potentiostat/Galvanostat model 283 at room temperature. Reductions CV of all compounds were performed in dichloromethane containing 0.1 M tetrabuty lammoniumhexafluorophosphate (Bu_4NPF_6) as the supporting electrolyte. The onset potential was determined from the intersection of two tangents drawn at the rising and background current of the cyclic voltammogram.

Computational Details

The geometrical and electronic properties were performed with the Amsterdam Density Functional (ADF) 2009.01 program package. The calculation was optimized by means of the B3LYP (Becke three parameters hybrid functional with Lee-Yang-Perdew correlation functionals with the 6-31G(d) atomic basis set. Then the electronic structures were calculated at τ-HCTHhyb/6–311++G(d, p) level. Molecular orbitals were visualized using ADF view.

Device Fabrication and Measurement

The EL devices were fabricated by vacuum deposition of the materials at a base pressure of 5×10^{-6} Torr onto glass precoated with a layer of indium tin oxide (ITO) with a sheet resistance of 20 Ω/square and transmissivity of 80% in blue light. Before deposition of an organic layer, the clear ITO substrates were treated with oxgen plasma for 5 min. The deposition rate of organic compounds was 0.9–1.1 Å s^{-1}. Finally, a cathode composed of LiF (1 nm) and aluminum (100 nm) was sequentially deposited onto the substrate in the vacuum of 10^{-5} Torr. The L–V–J of the devices was measured with a Keithley 2400 Source meter and PR655. All measurements were carried out at room temperature under ambient conditions

Synthesis

9-(3-(2-phenyl-1H-benzo[d]imidazol-1-yl) phenyl)-9H-carbazole (mNBICz)

A mixture of 1-(3-bromophenyl)-2-phenyl-1H-benzo[d]imidazole (2.78 g, 8.00 mmol), carba zole (1.5 g, 9 mmol), CuI (46 mg, 0.24 mmol), 18-crown-6 (64 mg, 0.24 mmol), K_2CO_3 (5.53 g, 40 mmol), and DMPU (5.0 mL) was refluxed under nitrogen for 48 h. After cooling, the mixture was extracted with CH_2Cl_2 and washed with the dilute HCl solution, and then the organic layer was dried over anhydrous Na_2SO_4. After removal of the solvent, the residue was purified by

column chromatography on silica gel using CH_2Cl_2 as the eluent to give a white powder. Yield: 88 %. ^{1}H NMR (400 MHz, $CDCl_3$) δ (ppm): 7.98 ~ 8.00 (d, 2H), 7.80 ~ 7.84 (d, 1H), 7.70 ~ 7.75 (t, 1H), 7.53 ~ 7.62(m, 4H), 7.32 ~ 7.48 (m, 4H), 7.15~7.30(m, 7H), 6.90 ~ 7.00 (s, 2H). ^{13}C NMR (400 MHz, $CDCl_3$) δ [ppm]: 152.55, 142.93, 140.48, 139.52, 138.63, 136.81, 131.98, 130.30, 129.96, 129.67, 128.77, 126.67, 125.98, 125.08, 123.73, 123.37, 120.20, 120.05, 110.58, 109.55. MS (APCI): *m/z* 436.1 $[M + H]^+$. Anal. calcd for $C_{31}H_{21}N_3$ (%): C 85.34, H 4.93, N 9.73; found: C 85.40, H 4.90, N 9.70

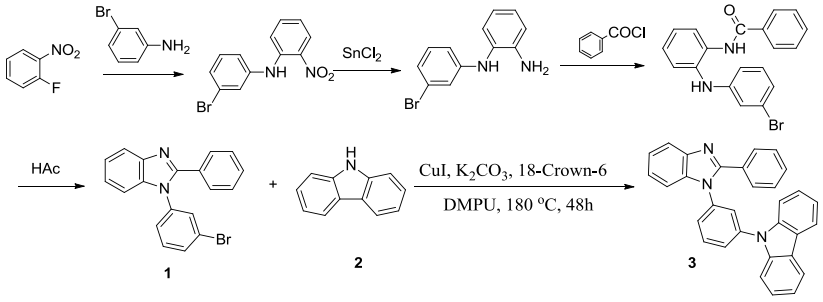

Scheme.S1 Synthetic procedure for **mNBICz**

Table S1 Photophysical properties and energy levels of mNBICz

T_g	T_d	PL (nm)	HOMO[a] (eV)	LUMO[b] (eV)	E_g[c] (eV)	E_T[d] (eV)
86℃	349.3 ℃	343, 360	-5.82	-2.55	3.57	2.78

List of figures

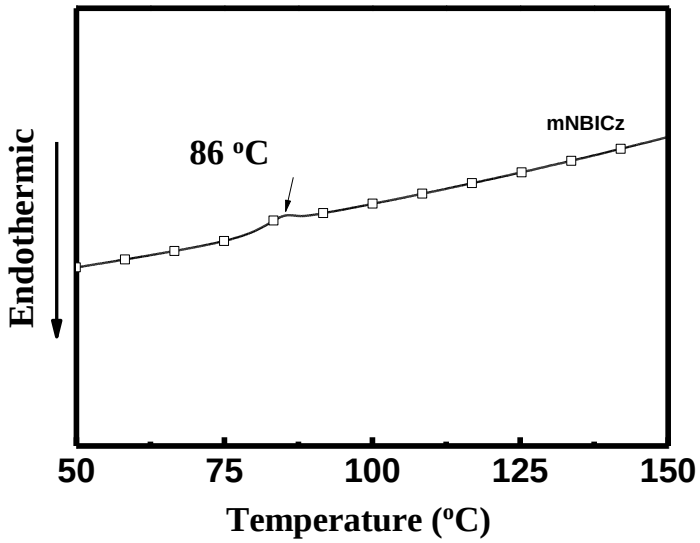

Fig.S1 DSC traces of the compounds **mNBICz** recorded at a heating rate of 10 ℃/min.

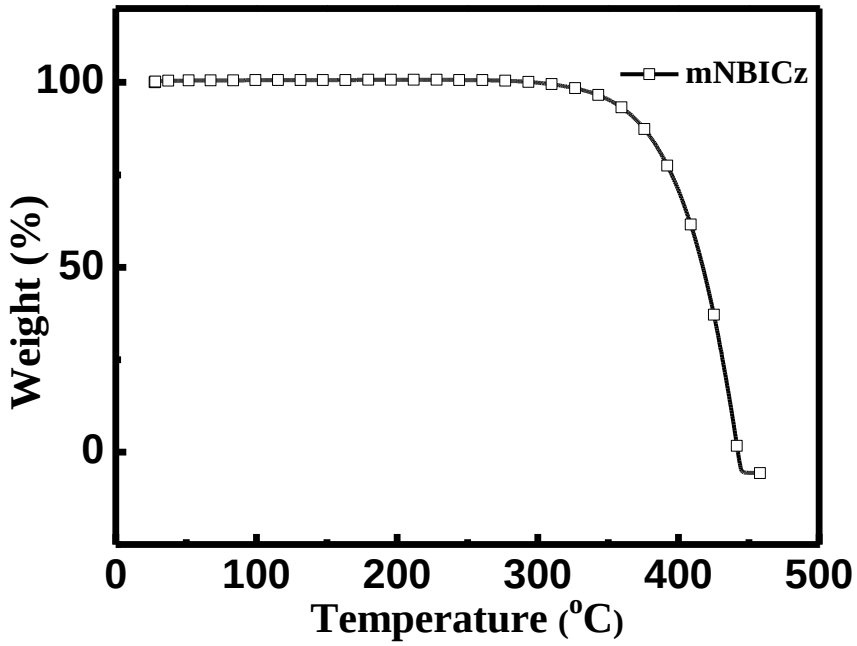

Fig.S2 TGA thermo-grams of the compounds **mNBICz** recorded at a heating rate of 10 ℃/min.

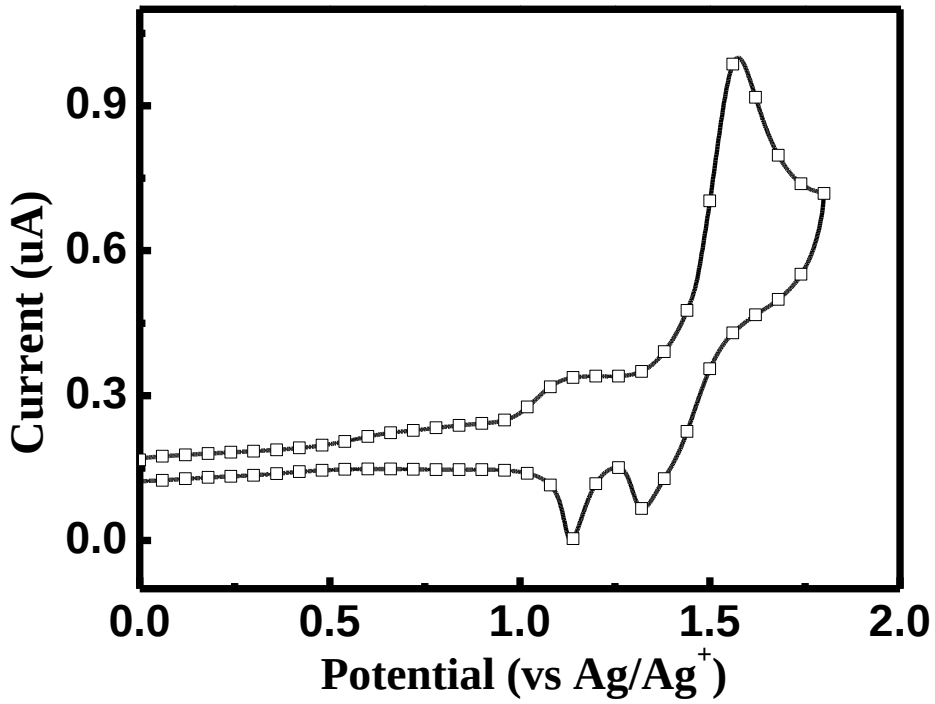

Fig.S3 CV curves of **mNBICz**. Working electrode: Pt button; reference electrode: Ag/Ag^+. Oxidation CV was performed in dichloromethane containing 0.1 M *n*-Bu_4NPF_6 as the supporting electrolyte at a scan rate of 100 mV/s.

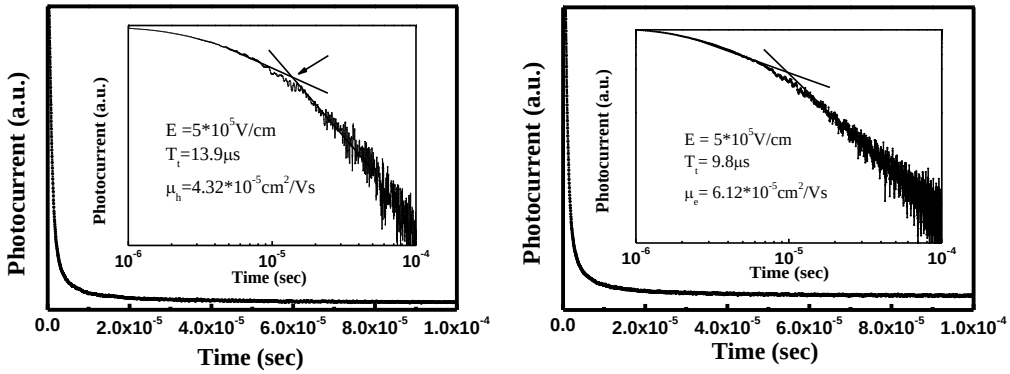

Fig.S4 log of the photocurrent vs. the log of time in a time-of-flight measurement. The electron and hole mobility (μ) was calculated from the values of the transit time (T_t), the sample thickness and the applied voltage (V) according to the equation $\mu = D^2/(VT_t)$.

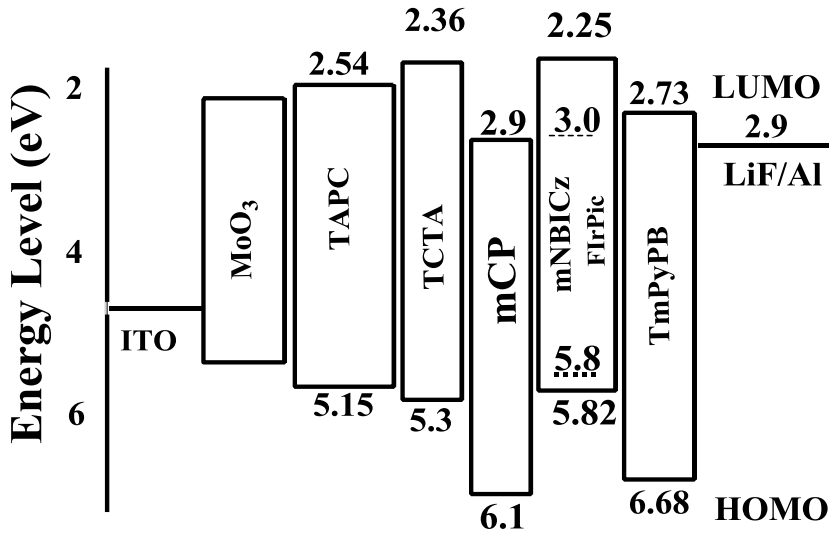

Fig.S5 the relative energy levels of the materials employed in the blue devices

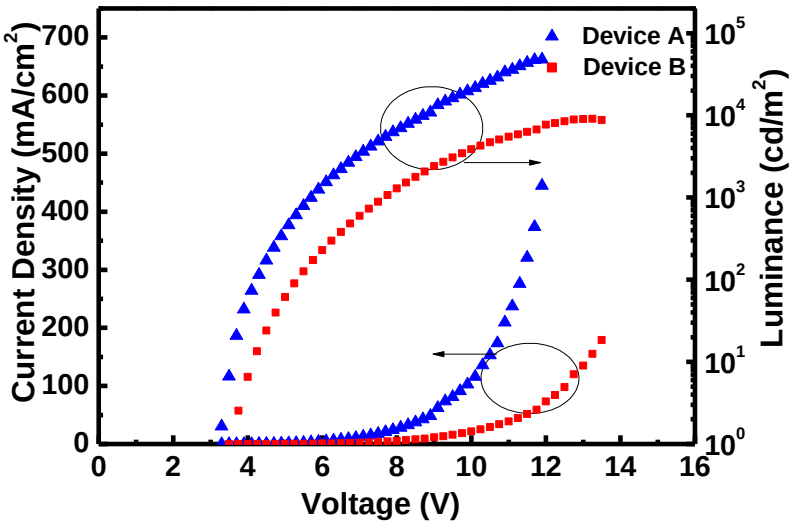

Fig.S6 Current density−voltage and luminance−voltage characteristics of the Device A and B

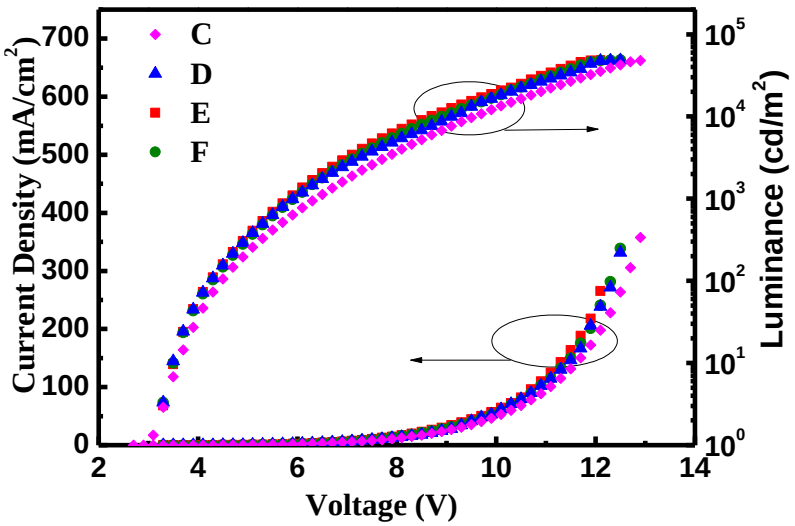

Fig.S7 Current density−voltage and luminance−voltage characteristics of the white Device C-F

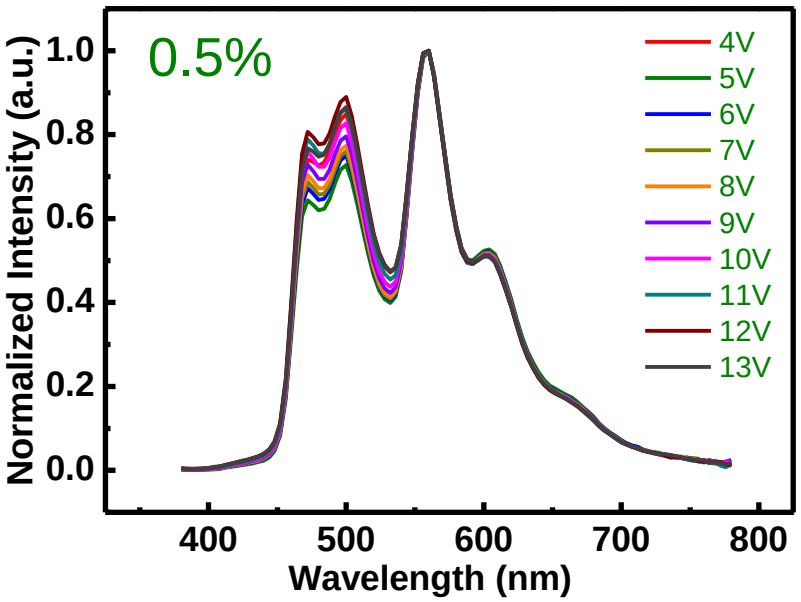

Fig.S8 EL spectrum of device C at different biases

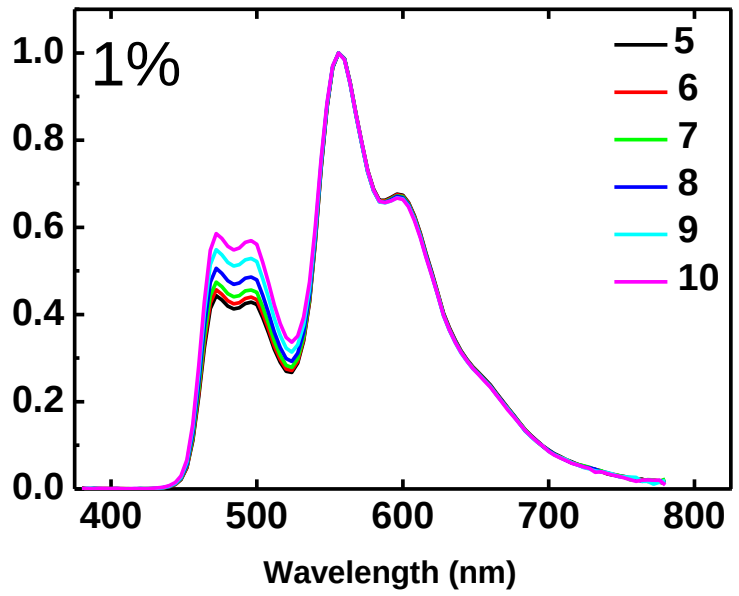

Fig.S9 EL spectrum of device D at different biases

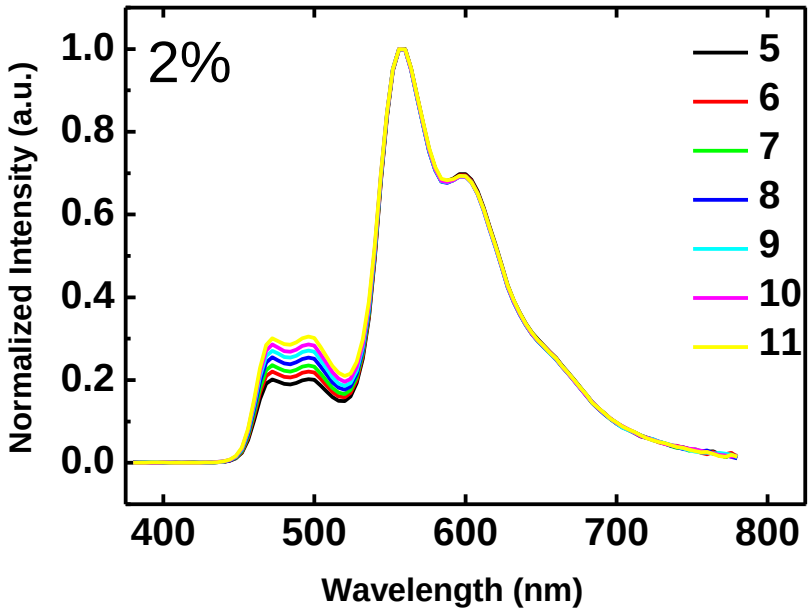

Fig.S10 EL spectrum of device F at different biases